Turbulence Modeling of Source and Sink Flows

Israt Jahan Eshita

Abstract—Flows developed between two parallel disks have many engineering applications. Two types of non-swirling flows can be generated in such a domain. One is purely source flow in disc type domain (outward flow). Other is purely sink flow in disc type domain (inward flow). This situation often appears in some turbo machinery components such as air bearings, heat exchanger, radial diffuser, vortex gyroscope, disc valves, and viscosity meters. The main goal of this paper is to show the mesh convergence, because mesh convergence saves time, and economical to run and increase the efficiency of modeling for both sink and source flow. Then flow field is resolved using a very fine mesh near-wall, using enhanced wall treatment. After that we are going to compare this flow using standard k-epsilon, RNG k-epsilon turbulence models. Lastly compare some experimental data with numerical solution for sink flow. The good agreement of numerical solution with the experimental works validates the current modeling.

Keywords—Hydraulic diameter, k-epsilon model, meshes convergence, Reynolds number, RNG model, sink flow, source flow and wall y+.

I. INTRODUCTION

THE flow produced within the gap formed by two flat disks has been examined intensively in the past. When the fluid enters into a centrally located cavity on one disc or both discs and drained out through the periphery is known as source flow in disc type domain (outward flow).On the other hand, when the fluid entered through the periphery and drained out by a centrally located cavity on one disc or both discs is known as sink flow in disc type domain (inward flow).
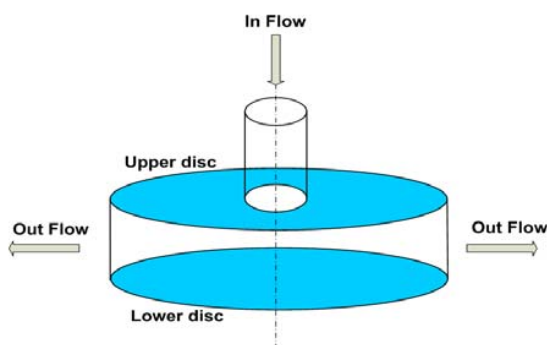

Fig. 1 Purely source flow in disc type domain (outward flow)

Israt Jahan Eshita is with the Mechanical Engineering Department, Concordia University, Montreal, Canada (phone: 4388284881; e-mail: i_eshita@encs.concordia.ca, eshita20b@ yahoo.com).
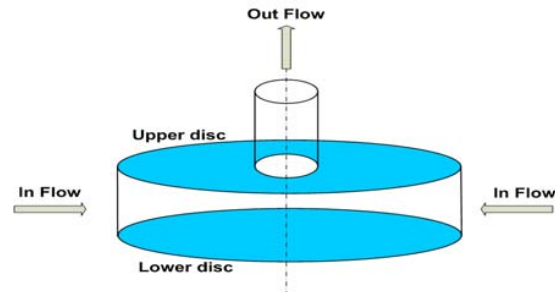
Fig. 2 Purely sink flow in disc type domain (inward flow)

At first glance, it seems that these two types of flows are fully reversible. But interestingly, it will soon become clear, that the two types of flows are not dramatically different. The velocity for both flows show the familiar Poiseuille's profile similar to that between two flat plates for extremely small local Reynolds numbers. Only under this special condition the two types of flow are fully reversible [1]. The inflow is characterized by persistence to remain laminar even at very high Reynolds numbers. This is because of the stabilizing effects of acceleration or to laminarize in case that the entering fluid is initially turbulent [2]. In this paper we are focusing on solutions to the steady, laminar radial flow between two flat disks where all material elements are either monotonically accelerating, or decelerating. Where the streamlines either converge, or diverge over the entire channel. The flow is symmetric about the mid-channel plane. For both flow cases, the results of the radial velocity are presented as functions of one non-dimensional parameter that combines the Reynolds number and the radial distance. There are many practical and industrial importances of these flows. Outward flow or source flow can be found in radial diffuser, air bearings, centrifugal compressor, VTOL aircraft with centrally located pointed jets, air-cushion vehicle (ACV). On the other hand inward flow or sink flow can be found in disc valves, flow rate and viscosity meters, thrust bearing. Swirling flow can be generated both outward and inward flows. The application of swirling flow in the industrial area is very essential.

A low Reynolds number k-epsilon model has been used to model the Reynolds stresses. According to the numerical study the acceleration parameter is not the only factor governing turbulent-laminar transition in this flow, the gap ratio also plays a significant role. The inward laminar flow between two disks has been studied by many investigators. In 1956 McGinn developed an expression for pressure distribution using the argument that the pressure variation is partly due to the inertial contribution and partly due to viscous dissipation [3]. A numerical solution to the radial inflow between two flat disks problem has been presented. The radial velocity distribution has been found, that is depending on one non-dimensional

parameter that combines the Reynolds number and the radial distance. Boundary layer characteristics are observed in the velocity. Moreover, the viscous contribution assumed a radial velocity distribution of a creeping flow [4]. When the Reynolds number increased, the velocity values near the mid-channel decreased accompanied by a flattening of its profile. If the Reynolds number increased further the flat region was seen to propagate towards the wall, reaching the expected constant value over the entire axial direction, as the value of the Reynolds number reaches infinity [5]. The radial velocity profile is seen larger near the disk surface as well as to be lower at the mid-plane and. Numerical solutions to the radial inflow between two flat disks is presented as well as compare the numerical value with some experimental result.

II. METHODOLOGIES AND NUMERICAL MODEL

The flow within two parallel discs is a 2D, axisymmetric, stationary as well as co-rotating parallel disk. Steady, incompressible turbulent sink and source flows are developed here. As a solver ANSYS FLUENT (12.1) is used here. Reynolds-averaged Navier-Stokes equations (RANS) are used. Two types of Turbulent model using in the paper one is Standard k-epsilon model and other is RNG (Re-Normalization Group) k-epsilon model.
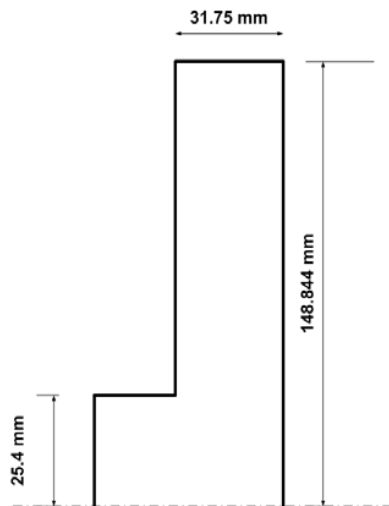

Fig. 3 Dimension of the geometry in 2D for symmetric half

Dimension and Description:

Radius of disc R: 148.844 mm.
Radius of sink exit / source inlet: 25.4 mm.
Gap between two discs H: 31.75 mm.
Hydraulic Diameter
For sink flow = 2H=2*31.75 = 63.5mm.
For source flow =25.4*2=50.8mm.
Air enters the cavity between two disks.
Density of air at inlet ρ=1.703236 kg/m^3.
Dynamic viscosity of air μ=2.29e-05 kg/m-s.
Mass flow rate of air = 0.094804 kg/s. (Source Flow).
Turbulence intensity I= 12% (Experimental value).

RANS-based turbulence models (Two equation turbulence models): Additional unknowns in Navier-Stokes equations due to averaging process.

Conservation of Mass:

$$\frac{\partial \rho}{\partial t} + \nabla.(\rho v) = 0 \qquad (1)$$

Conservation of Momentum:

$$\underbrace{\rho(\frac{\partial v}{\partial t})}_{\substack{Unsteady \\ acceleration}} + \underbrace{v.\nabla v}_{\substack{Convective \\ acceleration}} = \underbrace{-\nabla p}_{\substack{Pressure \\ gradient}} + \underbrace{\mu\nabla^2 v}_{Viscosity} + \underbrace{f}_{\substack{Other \\ forces}} \qquad (2)$$

Conservation of Reynolds Averaged Navier Stoke Equation:

$$\rho\frac{\partial \overline{u}_j\overline{u}_i}{\partial x_j} = \rho\overline{f}_i + \frac{\partial}{\partial x_j}\left[-\overline{p}\delta_{ij} + \mu\left(\frac{\partial \overline{u}_i}{\partial x_j} + \frac{\partial \overline{u}_j}{\partial x_i}\right) - \rho\overline{u_i'u_j'}\right] \qquad (3)$$

A. Standard k-Epsilon Model Equations

Two equation turbulence models are one of the most common types of turbulence model. By definition, two equation models include two extra transport equations to represent the turbulent properties of the flow. This allows a two equation model to account for history effects like convection and diffusion of turbulent energy.

1. The Transport Equations for k (Turbulent Kinetic Energy):

$$\frac{\partial}{\partial t}(\rho k) + \frac{\partial}{\partial x_i}(\rho k u_i) = \frac{\partial}{\partial x_j}\left[\left(\mu + \frac{\mu_t}{\sigma_k}\right)\frac{\partial k}{\partial x_j}\right] + P_k + P_b - \rho\in = -Y_M + S_k \quad (4)$$

2. The Transport Equations for Dissipation (Epsilon):

$$\frac{\partial}{\partial t}(\rho\in) + \frac{\partial}{\partial x_i}(\rho\in u_i) = \frac{\partial}{\partial x_j}\left[\left(\mu + \frac{\mu_t}{\sigma_\in}\right)\frac{\partial\in}{\partial x_j}\right] + C_{1\in}\frac{\in}{k}(P_k + C_{3\in}P_b) - C_{2\in}\rho\frac{\in^2}{k} + S_\in \quad (5)$$

B. RNG (Re-Normalization Group) k-Epsilon Model:

The RNG model was developed using Re-Normalization Group (RNG) methods to renormalize the Navier-Stokes equations, to account for the effects of smaller scales of motion [6]. In the standard k-epsilon model the eddy viscosity is determined from a single turbulence length scale, so the calculated turbulent diffusion is that which occurs only at the specified scale, whereas in reality all scales of motion will contribute to the turbulent diffusion. On the other hand RNG approach, which is a mathematical technique that can be used to derive a turbulence model similar to the k-epsilon, results in a modified form of the epsilon equation which attempts to account for the different scales of motion through changes to the production term. Using a simple interpretation where buoyancy is neglected. The turbulent viscosity is calculated in the same manner as with the standard k-epsilon model. The RNG k- epsilon model was derived using a rigorous statistical technique (called renormalization group theory). It is similar in form to the standard k- epsilon model, but includes the

following refinements: The RNG model has an additional term in its epsilon equation that significantly improves the accuracy for rapidly strained flows. The effect of swirl on turbulence is included in the RNG model, enhancing accuracy for swirling flows. The RNG theory provides an analytical formula for turbulent Prandtl numbers, while the standard k-epsilon model uses user-specified, constant values. While the standard k-epsilon model is a high-Reynolds-number model, the RNG theory provides an analytically-derived differential formula for effective viscosity that accounts for low-Reynolds-number effects. Effective use of this feature does, however, depend on an appropriate treatment of the near-wall region. These features make the RNG k- epsilon model more accurate and reliable for a wider class of flows than the standard k- epsilon model.

1. Mesh Convergence:

Mesh convergence is very important for quick solution and better result. Mesh convergence saves the time, and economical to run and increase the efficiency. When the mesh refined enough that the solution doesn't change significantly upon further mesh refinement, we can say mesh converse properly. We refine our mesh from course to fine, and refine the mesh near the discs walls. To get the more refine mesh we should increase the element number.

TABLE I
DETAILS INFORMATION ABOUT SIX DIFFERENT TYPES OF MESH

Number of Nodes	Number of elements	Maximum Grid Size (mm)	Minimum Grid Size (mm)	Minimum Aspect Ratio	Maximum Aspect Ratio
1516	1408	2	0.02	1	1.384
5271	5100	1.05	0.0105	1.0489	4.087
11276	**11025**	**0.7**	**0.007**	**1.0225**	**5.247**
15599	15300	0.6	0.006	1.0465	5.640
17684	17370	0.57	0.0057	1.0277	7.069
20859	20520	0.53	0.0053	1.0126	9.819

Table I shows us various properties of all meshes. The third mesh (11276 nodes) highlighted as blue because form this mesh, grid-independent or mesh convergence occurred. Continue calculation to convergence. Compare results obtained with different grids.
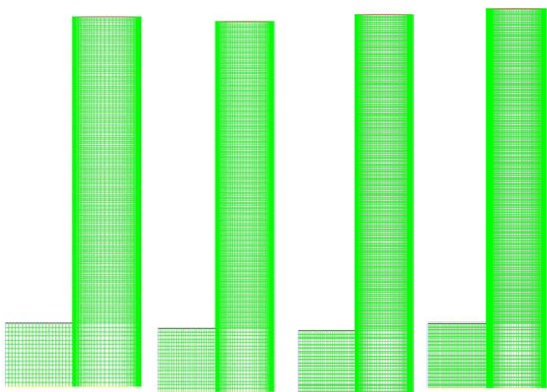

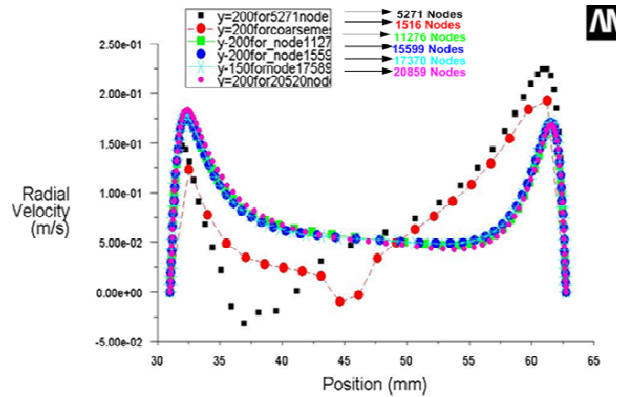
Fig. 4 Mesh refinement of 11276, 15599, 17589, 20520 Nodes

Fig. 5 Mesh Convergence for six different types mesh

For Fig. 5 we can observe that 1st and 2nd meshes are not conversed. But form 3rd to 6th meshes are properly conversed. So we can say that 3rd mesh (11276 nodes) refined enough that the solution doesn't change significantly upon further mesh refinement.

III. RESULTS AND DISCUSSION

We have to initialize the flow field using the boundary conditions set at velocity-inlet. After that run the calculation to set the iteration 500 for the Number of Iterations. The solution is converged after approximately 375 iterations. Here we use the 1st conversed mesh (11276 nodes) because it is economic and less time consuming.
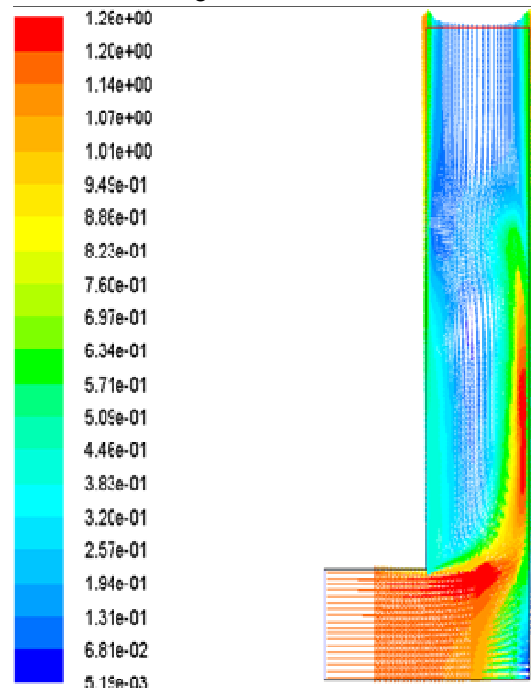

Fig. 6 Velocity Vectors (source flow) colored by Velocity Magnitude

From Fig. 6 velocity vector of source flow is shown. If we observed carefully there is something interesting thing happen that is, the magnified view of the velocity field displaying a

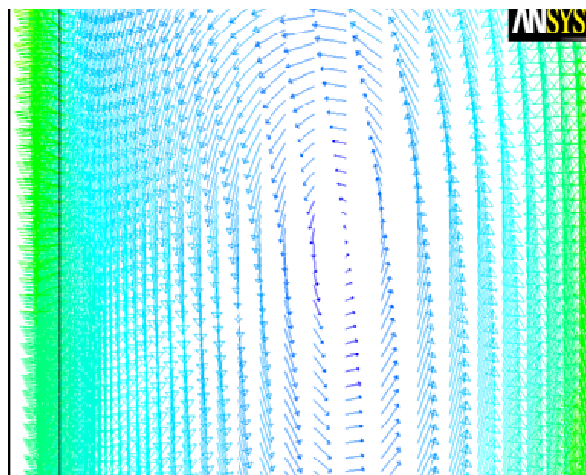counter-clockwise circulation of the flow is shown in Fig. 7.

Fig. 7 The magnified view of mid section of velocity vectors (source flow) colored by Velocity Magnitude

If we observe the Fig. 8 we can see the high pressure that occurs on the right disk near the hub because stagnation of the flow entering from the bore.

In this part we are focused on the velocity vector and pressure contour of sink and source flow. If we observed the velocity vector of sink and source flow shown in below, we can see from Fig. 9 that for the sink flow the highest velocity is located at the periphery of the discs. On the other hand, for source flow it is opposite phenomenon occurs, the highest velocity is the centrally located cavity.
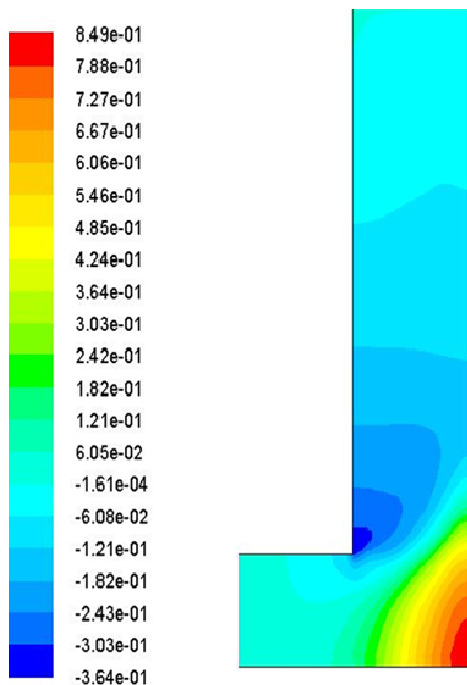

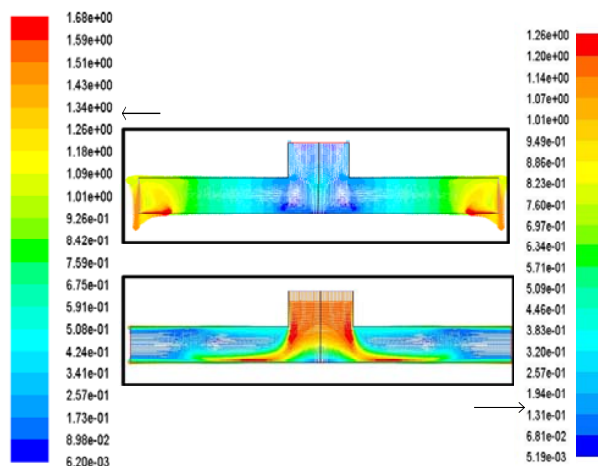Fig. 8 Contours of Static Pressure for the source flow

Fig. 9 Velocity Vectors of (top one) sink flow and (bottom one) source flow
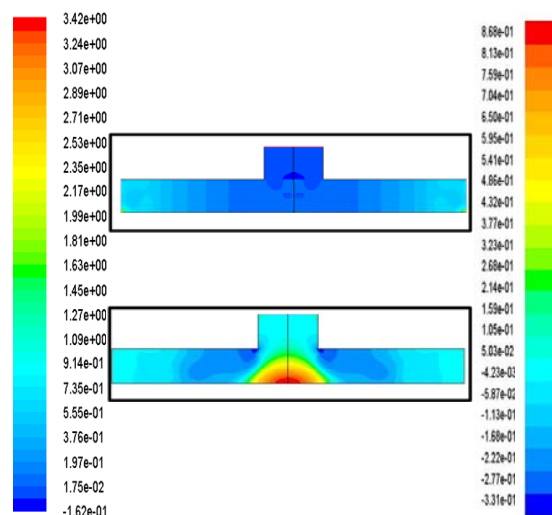

Fig. 10 Contours of static pressure (top one) sink flow and (bottom one) source flow

Fig. 10 shows us the contours of static pressure. If we observed carefully the first contours of sink flow we can see that for the sink flow the highest static pressure is located at the little area of periphery of the discs. On the other hand, for source flow it is opposite phenomenon occurs, the highest static pressure is located at the centrally located cavity.
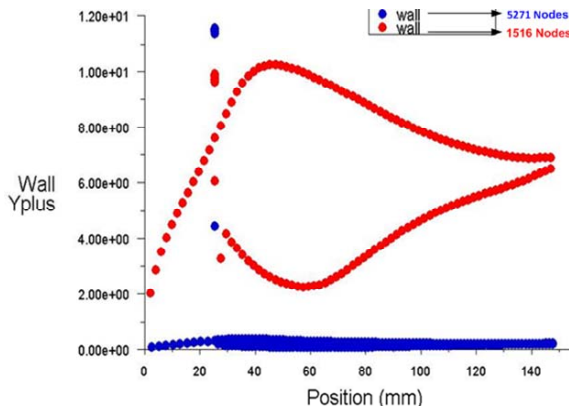
Fig. 11 Wall Yplus Distribution on 2 discs wall for 1516 nodes (coarse mesh) and first refine mesh 5271 nodes

Fig. 11 shows us the y plus distribution vs. distance of discs wall surface of 1516 nodes (coarse mesh) and first refine mesh 5271 nodes. The value of y plus for coarse mesh is 10, which is not expectable. But for 1st refine mesh it gives very low value of y plus, it is less than 1.
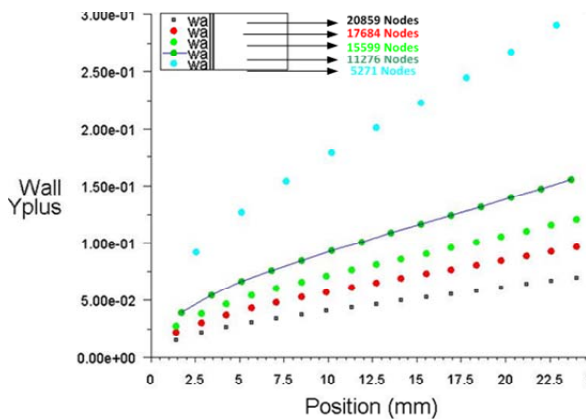

Fig. 12 Wall Yplus Distribution on 2 discs wall for coarse to five refine mesh

On the other hand Fig. 12 shows us various y plus values vs. distance of discs wall surface for refine mesh for 5271 nodes it gives about 0.3 y plus value, for 11276 nodes it gives 0.15 y plus value, for 15599 nodes it gives 0.125 y plus value, for 17684 nodes it gives 0.1 y plus value and 20859 nodes it gives 0.05 y plus value. So we can say that, the more we refine the wall of the dices the y plus value will be less. Ideally, while using enhanced wall treatment, the wall y+ should be in the order of 1 (at least < 5) to resolve viscous sub layer. So the plot strongly justifies the applicability of enhanced wall treatment to the given mesh.
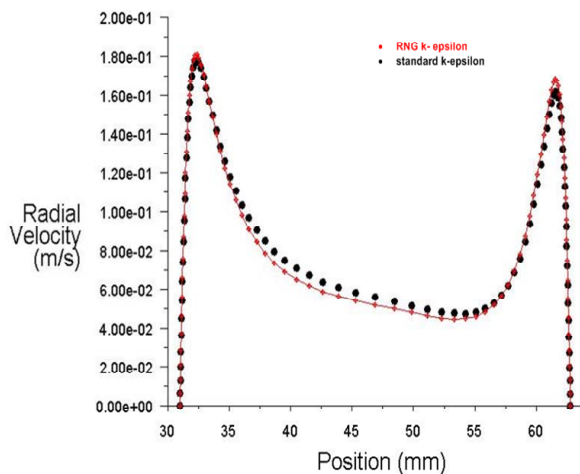

Fig. 13 Radial velocity vs. position between two dices for RNG k-epsilon and standard k-epsilon

From the above Fig. 13 we can observe that the peak velocity predicted by the RNG k-epsilon solution is higher than standard the k-epsilon. This is due to the less diffusive character of the RNG model than standard k-epsilon model.
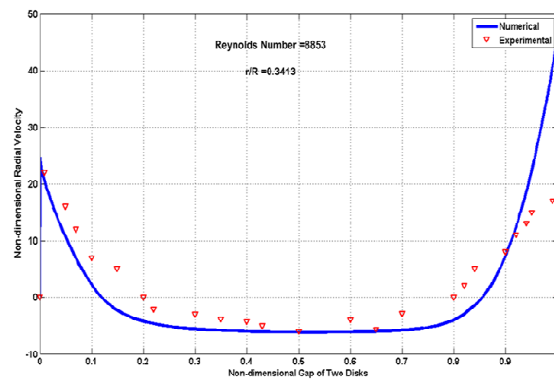

Fig. 14 Non-dimensional radial velocity vs. non-dimensional gap of two discs for experimental data with some numerical data for (RNG k-epsilon) solution

It is clear from the figures that the radial inflow occurs adjacent to the two discs surfaces. Near the wall we see spike of growing velocity. This is because, when fluid approaches the exit the effective flow area decreases so the flow must be experiencing an increase in the inward radial velocity. From the Fig. 14 we can observe that the numerical result is good match with experimental data. So we can say that, the numerical solution of (RNG k-epsilon) model gives us reasonable agreement between numerical result and the previous experimental works [6].
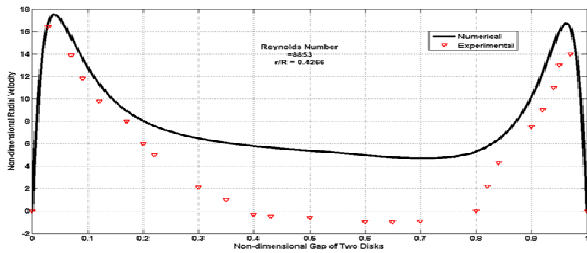
Fig. 15 Non- dimensional radial velocity vs. non-dimensional gap of two discs for experimental data with some numerical data for (standard k-epsilon) solution

On the other hand, from the Fig. 15 we can observe that the numerical result is match with experimental data in both disc wall but in the mid region there is some difference between the numerical result and the previous experimental works. This is because the standard k-epsilon model has not good effect of swirling flow. So for swirling dominant flow the result of standard k-epsilon is not good like RNG k-epsilon model.

IV. CONCLUSION

The numerical investigation of sink and source flow between the gaps of two discs was presented in this paper. The comparison between source flow (out ward flow) and sink flow (inward flow) as velocity vector and static pressure contour are also described. Grid independency or mesh convergence study is successful as well as mesh convergence saves the time, and economical to run and increase the efficiency. On the other hand y+ plot justifies the applicability of enhanced wall treatment. The value of y+ is less than 1 for all five refine meshes. From the experiment and numerical comparison, when we use RNG k-epsilon model it gives good result but for standard k-epsilon there is some problem in the mid –chamber of the graph, because standard k-epsilon model gives poor predictions for swirling and rotating flows. It becomes clear that near the disc walls the spike of the radial velocity are due to synergetic contribution of boundary layer development as well as reduction of the local cross sectional area. After all, we apply the method to approximate some experimental results which is useful for practical applications.

NOMENCLATURE

Vr = radial velocity component.
V_θ = tangential or swirling velocity component
Vz = axial velocity component
P = static pressure
Re = Reynolds number
μ = fluid dynamic viscosity
ρ = density of fluid
k = turbulence kinetic energy
G = aspect ratio of disc
H = gap between two discs
I = turbulence intensity
R = radius of disc
r = radius of centrally located cavity

ϵ = dissipation per unit mass
P_k = production of k
$\dot{m}$ = mass flow rate
Q = volume flow rate

REFERENCES

[1] Vatistas, G. H. G. Zitouni "Purely accelerating and decelerating flows within two flat disks" Acta Mechanica, Vol.123, 1997, pp 151-161.
[2] Murphy, H. D., Chambers, E W., McEligot, D. M.: Laterally converging flow. Part 1. Mean flow. J. Fluid Mech. 127, 379-401 (1983).
[3] A. Singh a, B.D. Vyas and U.S. Powle b "Investigations on inward flow between two stationary parallel disks" International Journal of Heat and Fluid Flow Vol.20, 1999, pp 395-401.
[4] Vatistas, G. H. "Radial flow within two flat disks". AIAA J. Vol 28, 1990, pp 1308-1310.
[5] Vatistas, G. H, A. Ghila, and G. Zitouni, "Radial inflow between two flat disks" Acta Mechanica Vol 113, 1995, pp 109 -118.
[6] Yakhot, V., Orszag, S.A., Thangam, S., Gatski, T.B. & Speziale, C.G. (1992), "Development of turbulence models for shear flows by a double expansion technique", Physics of Fluids A, Vol. 4, No. 7, pp1510-1520.